Plasmin Triggers a Switch-Like Decrease in Thrombospondin-Dependent Activation of TGF-β1

Lakshmi Venkatraman,[†‡] Ser-Mien Chia,[†] Balakrishnan Chakrapani Narmada,[§] Jacob K. White,[†**] Sourav S. Bhowmick,[†‡] C. Forbes Dewey, Jr.,[†††] Peter T. So,[†††] Lisa Tucker-Kellogg,[†‖*] and Hanry Yu[†§¶‖‡‡*]

[†]Singapore-MIT Alliance, Computational Systems Biology Programme, Singapore; [‡]School of Computer Engineering, Nanyang Technological University, Singapore; [§]NUS Graduate School for Integrative Sciences, Singapore; [¶]Department of Physiology and [‖]Mechanobiology Institute, Temasek Laboratories, National University of Singapore, Singapore; [**]Department of Electrical Engineering and Computer Science and [††]Department of Mechanical Engineering, Massachusetts Institute of Technology, Cambridge, Massachusetts; and [‡‡]Institute of Bioengineering and Nanotechnology, A*STAR, Singapore

ABSTRACT Transforming growth factor-β1 (TGF-β1) is a potent regulator of extracellular matrix production, wound healing, differentiation, and immune response, and is implicated in the progression of fibrotic diseases and cancer. Extracellular activation of TGF-β1 from its latent form provides spatiotemporal control over TGF-β1 signaling, but the current understanding of TGF-β1 activation does not emphasize cross talk between activators. Plasmin (PLS) and thrombospondin-1 (TSP1) have been studied individually as activators of TGF-β1, and in this work we used a systems-level approach with mathematical modeling and in vitro experiments to study the interplay between PLS and TSP1 in TGF-β1 activation. Simulations and steady-state analysis predicted a switch-like bistable transition between two levels of active TGF-β1, with an inverse correlation between PLS and TSP1. In particular, the model predicted that increasing PLS breaks a TSP1-TGF-β1 positive feedback loop and causes an unexpected net decrease in TGF-β1 activation. To test these predictions in vitro, we treated rat hepatocytes and hepatic stellate cells with PLS, which caused proteolytic cleavage of TSP1 and decreased activation of TGF-β1. The TGF-β1 activation levels showed a cooperative dose response, and a test of hysteresis in the cocultured cells validated that TGF-β1 activation is bistable. We conclude that switch-like behavior arises from natural competition between two distinct modes of TGF-β1 activation: a TSP1-mediated mode of high activation and a PLS-mediated mode of low activation. This switch suggests an explanation for the unexpected effects of the plasminogen activation system on TGF-β1 in fibrotic diseases in vivo, as well as novel prognostic and therapeutic approaches for diseases with TGF-β dysregulation.

INTRODUCTION

Transforming growth factor (TGF)-β1 is a multifunctional cytokine that regulates differentiation, apoptosis, migration, and wound healing. Defects in TGF-β1 signaling have been implicated in fibrotic diseases (1), diabetic nephropathy (2), cancer metastasis (3), and other diseases (4). TGF-β1 signaling is tightly regulated at many levels, and its intracellular modulation by the smad system is particularly well studied (5,6). The extracellular activation of TGF-β1 is important for regulating its action because TGF-β1 is secreted from cells in a latent form (latent transforming growth factor (LTGF)-β1) and stored in the extracellular matrix until activation, creating a temporal discontinuity between LTGF-β1 expression and active TGF-β1 function (7). Before secretion occurs, precursor TGF-β1 protein dimerizes and is noncovalently bound to an inactivating latency-associated peptide (LAP), which is further associated with the latent-TGF-β1 binding protein (LTBP). The latent complex is secreted by the cell and tethered to the extracellular matrix, but the latent form has no known function and does not bind with specific cell surface receptors (7,8). The active TGF-β1 dimer can be released from LAP inactivation by a variety of physical, chemical, and biological triggers, such as high temperature, acidic pH, reactive oxygen species, integrins, proteases (e.g., plasmin (PLS)), and the matrix protein thrombospondin-1 (TSP1) (7,8).

TSP1 is a large, matricellular glycoprotein that is produced by different cell types and has important roles in cell attachment, angiogenesis, inflammation, and fibrosis (9). TSP1 is an important activator of TGF-β1 in vivo (10), and experiments that antagonized TSP1 with antisense therapy or inhibitory peptides (11,12) caused a decrease in active TGF-β1 and improvements in fibrotic disease progression. The interaction between TSP1 and TGF-β1 is an autocrine mechanism in which TSP1 increases activation of TGF-β1, and TGF-β1 in turn increases TSP1 gene expression (13,14).

TGF-β1 can also be activated by proteases such as PLS, which cleave LAP (15). PLS is a broad-spectrum serine protease that participates in many aspects of injury response, including inflammation, dissolution of clots, angiogenesis, and remodeling of extracellular matrix. Hepatocytes are the main producers of plasminogen (PLG) (16), the precursor form of PLS, and PLG is converted to PLS by urokinase-type PLG activator (UPA). UPA is the predominant PLG activator in tissues (17,18) and its activity is inhibited by plasminogen-activator inhibitor 1 (PAI-1) (19). Contrary to expected results, in vivo perturbations of the PLS pathway components by overexpression of UPA (20) or knockout of PAI-1 (21) caused a significant decrease

Submitted November 2, 2011, and accepted for publication June 28, 2012.

*Correspondence: phsyuh@nus.edu.sg or LisaTK@nus.edu.sg

Editor: Andre Levchenko.

© 2012 by the Biophysical Society

0006-3495/12/09/1060/9 $2.00

http://dx.doi.org/10.1016/j.bpj.2012.06.050

(rather than an increase) in active TGF-β1. Previous work has not explained why PLS can activate TGF-β1 in isolation but can decrease TGF-β1 signaling in vivo. Here, we addressed this problem using a combination of mathematical modeling and experiments.

Individually, the PLS and TSP1 pathways of TGF-β1 activation are well understood; however, to our knowledge, this is the first study to examine these pathways in combination to better understand TGF-β1 regulation. A systems-level approach with mathematical modeling can address the cross talk between the PLS and TSP1 pathways of TGF-β1 activation. PLS is a broad-specificity protease that can cleave many matrix proteins, including TSP1 (22,23). A significant antagonism between TSP1 and PLS in a cellular context could create an interesting interplay between the two activation pathways. Mathematical modeling has been used to study emergent behaviors of systems, as well as to model different aspects of TGF-β1 intracellular signaling, such as TGF-β1 receptor dynamics (24), smad signaling (5), and nuclear smad shuttling (6). Computational modeling is particularly useful for elucidating bifurcations, qualitative changes in pathway behavior, and emergent behaviors that arise in a complex system (25–27). Bistability, or the presence of two stable steady states, explains how a robust and synchronized binary decision emerges in cell-cycle control and apoptosis (28). In previous work, we showed that activation of PLS by UPA is capable of displaying bistability in models and in vitro (29).

In this work, we constructed a mathematical model including both PLS and TSP1 to obtain a systems-level perspective of the role of PLS in TGF-β1 activation. In the computational model, TGF-β1 exhibited a switch-like bistable response to PLS, decreasing from a high level of active TGF-β1 to a low level of active TGF-β1 with increasing doses of PLS. We experimentally tested key predictions of the model and confirmed them using rat liver cell types that naturally express the relevant proteins. Experimental measurements confirmed that increasing the availability of PLS caused a switch-like decrease in activation of TGF-β1. We conclude that TGF-β1 activation can be maintained at a high level by a TSP1-predominant mode of activation, or at a lower level by a PLS-predominant mode of activation. Bistable switching of TGF-β1 activation constitutes a novel and potentially robust mechanism for regulating TGF-β1 function.

MATERIALS AND METHODS

Computational modeling

Ordinary differential equations (Table S1 in the Supporting Material), constructed from the reaction equations in Table 1, were simulated with the ODE15s stiff solver in MATLAB (The MathWorks, Natick, MA; www.mathworks.com). Although linear terms, instead of the more-complex Michaelis-Menten kinetics, are assumed because the k_M parameters are much higher than substrate concentrations (30–32), this assumption does not affect the outcome of bistable predictions (Fig. S1). A total of 100 random initial concentration of all species, between 1 nM and 0.36 μM, were generated using Latin Hypercube sampling (33,34) and simulated until a steady state was reached. To construct steady-state plots with respect to parameter variation, we simulated model equations until convergence was seen (in 5000 steps).

Bistability in the model was tested with the use of going-up and coming-down simulations as described previously (29,33,34). For the going-up simulations (see Fig. 3 *A*, *solid curves*), a specified parameter of the model was perturbed over a range of values. For each value of the parameter, the system was initialized in a state with TGF-β1 low, and then simulated until a steady state was achieved. For the coming-down simulations (see Fig. 3 *A*, *dashed curves*), the same range of parameter values was tested, except that for each coming-down test, the system was initialized with TGF-β1 high. The test was positive for bistability if it revealed a range of parameter values for which the going-up and coming-down simulations yielded two different steady states.

Bifurcation diagrams were performed using XPPAUT (www.math.pitt.edu/~bard/xpp/xpp.html). For a robustness analysis (see Fig. 4 *B*), 100 random parameter vectors were generated using Latin-hypercube sampling (33,34) with $\pm 20\%$ to $\pm 50\%$ perturbation of the parameters from the nominal values. We calculated the number of parameter sets that were capable of bistability using the going-up and coming-down simulations. A parameter set was considered bistable if the difference between the high and low steady states of PLS was >0.35 μM. Note that 0.1 nM and 0.365 μM are the two steady states of PLS obtained from the Table 2 model simulations. For

TABLE 1 List of mass equations and parameters used for model construction

Reaction number	Reaction equation	Reaction number	Reaction equation
1	$scUPA + PLG \xrightarrow{keff_1} PLS + scUPA$	9,10	$TSP1 + PLS \underset{k_{-3}}{\overset{k_3}{\rightleftharpoons}} TSP1 : PLS$
2	$PLS + scUPA \xrightarrow{keff_2} tcUPA + PLS$	11	$TSP1 : PLS \xrightarrow{k_4} PLS$
3	$tcUPA + PLG \xrightarrow{keff_3} PLS + tcUPA$	12,13	$A2M + PLS \underset{k_{-5}}{\overset{k_5}{\rightleftharpoons}} A2M : PLS$
4	$PLS + LTGF\ \beta1 \xrightarrow{k_1} TGF\ \beta1 + PLS$	14,15	$PAI1 + tcUPA \underset{k_{-6}}{\overset{k_6}{\rightleftharpoons}} PAI1 : tcUPA$
5	$TSP1 + LTGF\ \beta1 \xrightarrow{k_2} TGF\ \beta1$	16,17	$PAI1 + scUPA \underset{k_{-7}}{\overset{k_7}{\rightleftharpoons}} PAI1 : scUPA$
6	$LTGF\ \beta1 \xrightarrow{k_{others}} TGF\ \beta1$	production	$\xrightarrow{\alpha_1} (scUPA;\ LTGF\ \beta1;\ A2M); \xrightarrow{\alpha_2} (PLG)$
7	$TGF\ \beta1 \xrightarrow{kp_1} TSP1$	degradation	$\{scUPA, tcUPA, PLS\} \xrightarrow{\mu_{edeg}}$; {all other protein species} $\xrightarrow{\mu_{pdeg}}$
8	$TGF\ \beta1 \xrightarrow{kp_2} PAI1$		

Reaction numbers correspond to the numbered arrows in Fig. 1 *A*, except for production and degradation, which are not numbered.

TABLE 2 Parameters and references for the PLS-TSP1-mediated TGF-β1 activation model

Reaction equation terms	Parameters	References
$v_1 = keff_1*[scUPA]*[PLG]$	$keff_1 = 0.035\ \mu M^{-1}s^{-1}$	(30)
$v_2 = keff_2*[PLS]*[scUPA]$	$keff_2 = 0.35\ \mu M^{-1}s^{-1}$	(30)
$v_3 = keff_3*[tcUPA]*[PLG]$	$keff_3 = 1.4\ \mu M^{-1}s^{-1}$	(30)
$v_4 = k_1*[PLS]*[LTGF\beta1]$	$k_1 = 0.035\ \mu M^{-1}s^{-1}$	(55)
$v_5 = k_2*[TSP1]*[LTGF\beta1]$	$k_2 = 24.5\ \mu M^{-1}s^{-1}$	(55)
$v_6 = k_{others}*[LTGF\beta1]$	$k_{others} = 0.005\ s^{-1}$	Variable
$v_7 = kp_1*[TGF\beta1]$	$kp_1 = 0.35\ s^{-1}$	Variable
$v_8 = kp_2*[TGF\beta1]$	$kp_2 = 1.05\ s^{-1}$	Variable
$v_9 = k_3*[TSP1]*[PLS]$	$k_3 = 17.5\ \mu M^{-1}s^{-1}$	(23)
$v_{10} = k_{-3}*[TSP:PLS]$	$k_{-3} = 0.0245\ s^{-1}$	(23)
$v_{11} = k_4*[TSP:PLS]$	$k_4 = 0.35\ \mu M^{-1}s^{-1}$	(23)
$v_{12} = k_5*[A2M]*[PLS]$	$k_5 = 24.5\ \mu M^{-1}s^{-1}$	(56)
$v_{13} = k_{-5}*[A2M:PLS]$	$k_{-5} = 0.0105\ s^{-1}$	(56)
$v_{14} = k_6*[tcUPA]*[PAI1]$	$k_6 = 0.035\ \mu M^{-1}s^{-1}$	(39)
$v_{15} = k_{-6}*[tcUPA:PAI1]$	$k_{-6} = 0.0035\ s^{-1}$	(39)
$v_{16} = k_7*[scUPA]*[PAI1]$	$k_7 = 0.07\ \mu M^{-1}s^{-1}$	(39)
$v_{17} = k_{-7}*[scUPA:PAI1]$	$k_{-7} = 0.0035\ s^{-1}$	(39)
$v_{18} = k_8*[TSP:PLS]$	$k_8 = 24.5\ s^{-1}$	Variable
$v_{19} = k_9*[TGF\beta1]$	$k_9 = 0.21\ s^{-1}$	(24)
μ_{edeg}	$\mu_{edeg} = 0.0525\ s^{-1}$	(57,58)
μ_{pdeg}	$\mu_{pdeg} = 0.0175\ s^{-1}$	(56,59)
α_1	$\alpha_1 = 0.0035\ s^{-1}$	(58,60)
α_2	$\alpha_2 = 0.035\ s^{-1}$	(58,60)
[scUPA, PLG, A2M, LTGFβ1]	[1 nM, 3 nM, 5 nM, 1 nM]; all other species had an initial concentration of 0 nM	(61,62)

Term v_i denotes the velocity of the reaction corresponding to the arrow labeled i in Fig. 1 *A*. Complete differential equations appear in Table S1. Parameters listed as variable were not available from the literature, so we instead provide values that are capable of inducing bistability in the system. The last row indicates the initial concentrations used for simulations.

Fig. 4 *C*, the parameter of interest was fixed while all others parameters were randomly perturbed by $\pm 20\%$ or $\pm 50\%$ from the nominal values.

RESULTS

Construction of the computational model

We constructed a computational model of PLS- and TSP1-mediated activation of TGF-β1 based on findings in the literature (Fig. 1). PLS activates TGF-β1 from LTGF-β1 through cleavage (15), whereas TSP1 activates TGF-β1 by binding to LTGF-β1 and causing a conformational change (7,36). Active TGF-β1 exerts regulation over PLS and TSP1 through gene expression. TGF-β1 is known to positively regulate TSP1 synthesis (13,14). TSP1 and TGF-β1 have an autocrine mechanism in which active TGF-β1 increases TSP1 expression, and more TSP1 protein increases the activation of LTGF-β1. TGF-β1 also maintains a negative regulation over PLS by gene expression of PAI-1 (37). PAI-1 is an inhibitor of both single-chain urokinase plasminogen activator (scUPA) and two-chain urokinase plasminogen activator (tcUPA) (38,39). Production of PLS from the inactive precursor PLG is initiated by scUPA, which nicks at the Arg^{560}-Val^{561} bond of PLG (30,40).

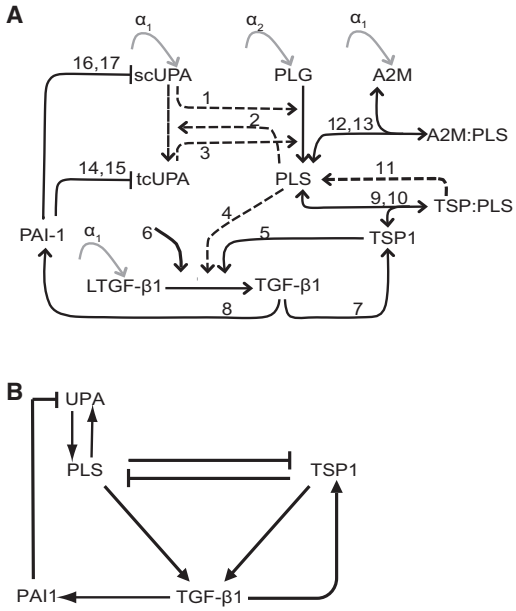

FIGURE 1 Model of PLS-mediated TGF-β1 activation. (*A*) Protein interaction network depicting the interactions between species. Gray arrows denote production; dotted arrows denote catalysis. Numbers on arrows correspond to the reaction equations in Table 1 and to the subscripts of terms in Table 2 and Table S1. (*B*) Schematic of the interactions between the main species of the model.

scUPA is a zymogenic precursor with little enzymatic activity, but once it activates PLS, PLS can cleave scUPA to the fully active tcUPA, which has higher catalytic efficiency. Also included in the computational model is α-2-macroglobulin (A2M), which is a specific inhibitor of PLS activity (41). Finally, interactions of mutual antagonism occur between PLS and TSP1, in which PLS degrades TSP1 (22), and TSP1 inhibits PLS (23,42). When PLS and TSP1 form a complex, two reactions are possible: the complex may be degraded or PLS may cleave TSP1 (equivalent in the model to degrading TSP1). Activation of TGF-β1 by integrins and all other mechanisms was treated as a single pooled reaction labeled "other". Synthesis of precursor proteins and inactive LTGF-β1 was provided at a constant rate. All of these known phenomena were incorporated to form the interaction network in Fig. 1 *A*. The reaction equations are shown in Table 1. Rate parameters were adapted from the literature when available, and unknown rates were estimated as shown in Table 2. The ordinary differential equations are listed in Table S1. Fig. 1 *B* shows a simplified schematic highlighting the interplay between the activators (i.e., TSP1 and PLS).

PLS negatively regulates TGF-β1 activation

To explore model steady states for different initial conditions, the model was simulated from 100 random initial conditions of all species. PLS concentrations, followed

over time, revealed convergence to two steady states, depending on the starting concentration of the species (Fig. 2 *A*). To test whether transition between the two steady states was ultrasensitive, simulations were performed with different values of PLS catalytic efficiency ($keff_2$) but with constant initial conditions. With increasing $keff_2$ values (i.e., increased proteolytic activity of PLS), PLS steady-state levels were seen to switch from a lower to a higher concentration (Fig. S2), whereas TGF-β1 (Fig. 2 *B*) and TSP1 (Fig. 2 *C*) decreased from higher to lower steady states. The change of steady states was ultrasensitive, meaning that small changes in $keff_2$ were able to cause abrupt shifts between protein steady states. Increasing PLS $keff_2$ caused a decrease in the steady-state level of TSP1 (Fig. 2 *C*). The inverse correlation between TSP1 and PLS can be explained by the antagonistic interaction between these two proteins (Fig. 1 *A*). However, increasing PLS efficiency also caused a decrease in active TGF-β1 levels (Fig. 2 *B*), and this inverse relationship is interesting because it suggests that although PLS is an activator of TGF-β1, increased PLS activity can cause a counterintuitive decrease in active TGF-β1 levels. These results indicate the presence of a threshold in PLS-mediated TSP1 inhibition, because only $keff_2$ values $> 0.6\ \mu M^{-1}s^{-1}$ were capable of inhibiting TSP1. Once over this threshold, PLS could inhibit TSP1 and break the positive feedback between TSP1 and TGF-β1, causing a net decrease in active TGF-β1 levels.

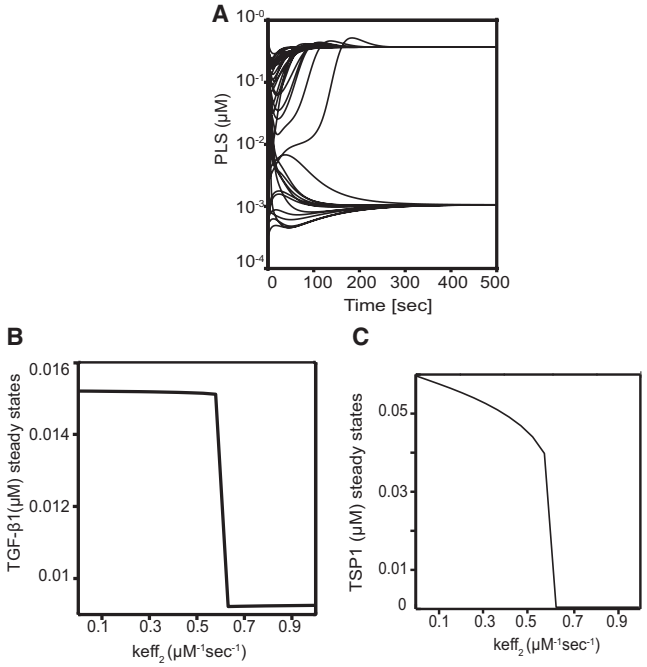

FIGURE 2 Model simulations. (*A*) The computational model was simulated in MATLAB using random values (0.2 nM to 0.2 μM) for all species, and PLS concentration was plotted over time. (*B* and *C*) The steady-state values of (*B*) TGF-β1 and (*C*) TSP1 are plotted as a function of $keff_2$.

Bistability and bifurcation analysis of the model

Preliminary simulations (Fig. 2) indicated that the parameter perturbations were capable of inducing a switch-like transition of system species. To test whether the ultrasensitive model is capable of displaying bistability, we conducted simulations to determine whether the steady state of the system depended on the initial conditions, with going-up and coming-down simulations (33,34) performed using the parameter $keff_2$. The model was initialized with high TGF-β1 (coming-down; *dashed line* in Fig. 3 *A*), and simulated with different values of $keff_2$. As expected, a rate of $keff_2 > 0.6\ \mu M^{-1}s^{-1}$ caused a switch in TGF-β1 levels from a higher to a lower steady state. Next, the model was initialized with low concentrations of TGF-β1 (going-up; *solid line* in Fig. 3 *A*) and simulated with different values of $keff_2$. Interestingly, the system retained the low steady state of TGF-β1 for values of $keff_2$ significantly $> 0.6\ \mu M^{-1}s^{-1}$. Models with $keff_2$ between $0.15\ \mu M^{-1}s^{-1}$ and $0.65\ \mu M^{-1}s^{-1}$ exhibited two different steady states of TGF-β1, depending on whether they had been initialized with low or high levels of TGF-β1. This indicates hysteresis, because the system retains a memory of its state despite changes in the stimulus (i.e., $keff_2$). The simulations therefore show that the TGF-β1 activation model is capable of displaying bistability, depending on the rate parameters.

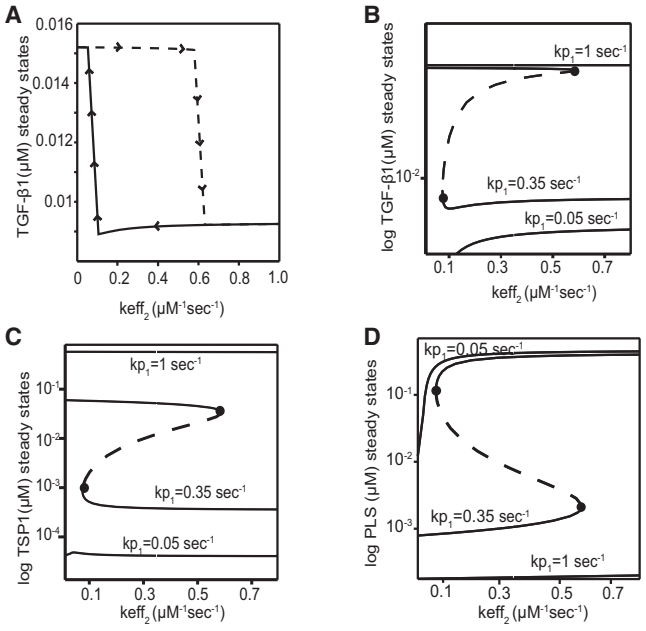

FIGURE 3 Bistability and bifurcation analysis. (*A*) Going-up and coming-down simulations were done for a range of $keff_2$ parameter values, and TGF-β1 steady-state levels are plotted. The dashed line indicates the coming-down curve with high initial concentrations of TGF-β1. The solid line indicates the going-up curve with low initial concentrations of TGF-β1. (*B–D*) Effects of two-parameter ($keff_2$ and kp_1) perturbations on (*B*) TGF-β1, (*C*) TSP1, and (*D*) PLS steady-state values. Solid black lines indicate stable steady-state solutions, and dotted lines indicate unstable steady states. Black dots indicate saddle node bifurcations.

In light of the molecular-level antagonism between PLS and TSP1, we studied the impact on bistability of simultaneously varying parameters for PLS and TSP1. We selected the PLS catalytic efficiency parameter, $keff_2$, and the positive feedback signal parameter, kp_1 (the gene expression of TSP1 induced by TGF-β1), and performed a parameter bifurcation analysis on kp_1 and $keff_2$ by individually modifying kp_1 parameter values over a range of $keff_2$ values. For $kp_1 = 0.05\ s^{-1}$ (i.e., low values of the positive feedback and little induction of TSP1), the system had a single steady state (monostable), with TGF-β1 (Fig. 3 *B*) and TSP1 (Fig. 3 *C*) maintained at a lower concentration and PLS maintained at a high concentration (Fig. 3 *D*). Conversely, when the kp_1 feedback signal strength was increased ($kp_1 = 1\ s^{-1}$), there was enough TSP1 to cause inhibition of PLS, and the system converged without bistability, for the entire range of $keff_2$ values, toward a single steady state with high levels of TSP1 and TGF-β1, and low levels of PLS. For intermediate values of kp_1 (e.g., $kp_1 = 0.35\ s^{-1}$), the system was bistable, as indicated by the presence of two saddle node bifurcation points (*black dots* in Fig. 3, *B–D*). For any value of $keff_2$ between these two saddle nodes (on the curve for $kp_1 = 0.35\ s^{-1}$), the resulting system has two stable fixed points and one unstable fixed point in between. To be capable of bistability, the system must therefore have some degree of balance between the parameters defining the TSP1 strength and the parameters defining the PLS strength. In addition to the TSP1-TGF-β1 positive feedback, there is a positive feedback loop between PLS and UPA (defined by $keff_3$) that also regulates bistability. Fig. S3 shows that the system is monostable for low values of $keff_3$ and kp_1, and bistable (shaded area within the cusp) for higher values of $keff_3$ and kp_1.

Because bistability depends on the parameter values, we next analyzed the robustness of the bistability to parameter variation. A two-parameter bifurcation diagram (Fig. 4 *A*) shows that the region of bistability (*shaded region* within the cusp) is large even when kp_1 and $keff_2$ are varied simultaneously. The shaded region inside the cusp represents models with bistability, and the boundary lines represent saddle node bifurcations. We next generated 100 parameter sets with a $\pm 20\%$ to $\pm 50\%$ variation from nominal values of all parameters listed in Table 2 (see Materials and Methods). For each parameter set, bistability was tested with going-up and coming-down simulations (43). Fig. 4 *B* shows the percent bistability, i.e., the proportion of parameter sets that are capable of bistability when all the parameters are varied. There is a ~2.5-fold decrease in bistable parameter sets, with a $\pm 50\%$ variation from the nominal value (Fig. 4 *B*), although >25% of the parameter sets are still capable of displaying bistability (Fig. 4 *C*). This suggests than many physiologically reasonable perturbations of the model, such as changes in protein synthesis rates, would be capable of creating or maintaining bistability.

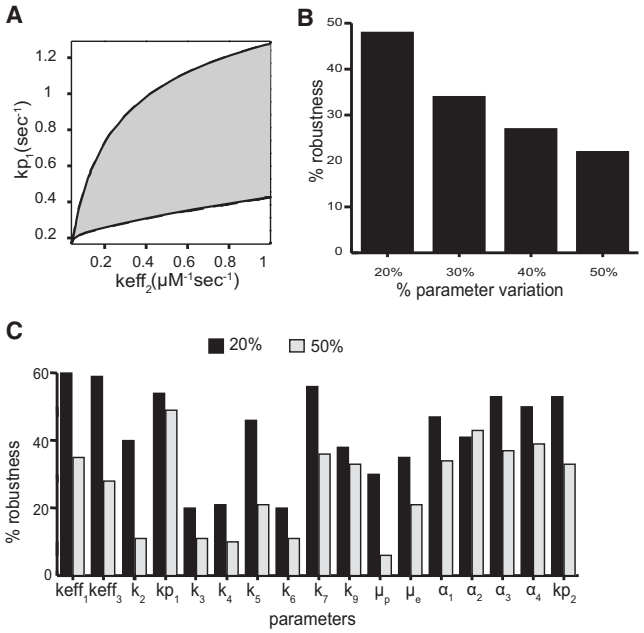

FIGURE 4 Robustness in bistability. (*A*) Two-parameter bifurcation diagram of TGF-β1 steady state when parameters kp_1 and $keff_2$ are modified simultaneously. The shaded portion represents the bistable area. (*B*) Using parameter vectors generated with $\pm 20\%$ to $\pm 50\%$ random variation from the nominal parameters, we calculated the percentage of models that retained bistability using $keff_2$ as the bifurcation parameter. (*C*) Percent robustness of bistability when each parameter is perturbed individually (see "Computational methods").

PLS causes a switch-like decrease in TGF-β1 activation in coculture

In a system with proteolysis, protein dynamics must be studied in the presence of production and turnover, because otherwise, inevitable proteolysis would preclude any interesting dynamical behaviors. It is easy to produce multiple proteins simultaneously in a theoretical model; however, PLG and TSP1 are normally secreted by different cell types, and typical cell cultures cannot provide a physiologically relevant dynamic between PLS and TSP1. We chose to test specific model-based predictions using a coculture of primary rat hepatocytes (liver epithelial cells) and rat T6 hepatic stellate cells (T6-HSC, liver fibroblasts). Hepatocytes and HSCs occur together in vivo and have frequently been cocultured to study injury response in vitro (44,45). Hepatocytes are the main producers of PLG in vivo (16), and we selected freshly isolated primary hepatocytes because they provide constant production of PLG as modeled. Similarly, T6-HSCs provide strong production of TSP1 and LTGF-β1. An HSC-predominant coculture has a higher ratio of T6-HSC to hepatocytes, and shows high production of TSP1 and low production of PLG.

To test the effect of PLS on TGF-β1 activation, we established HSC-predominant cocultures (see Supporting Material) and administered different levels of PLG. Because

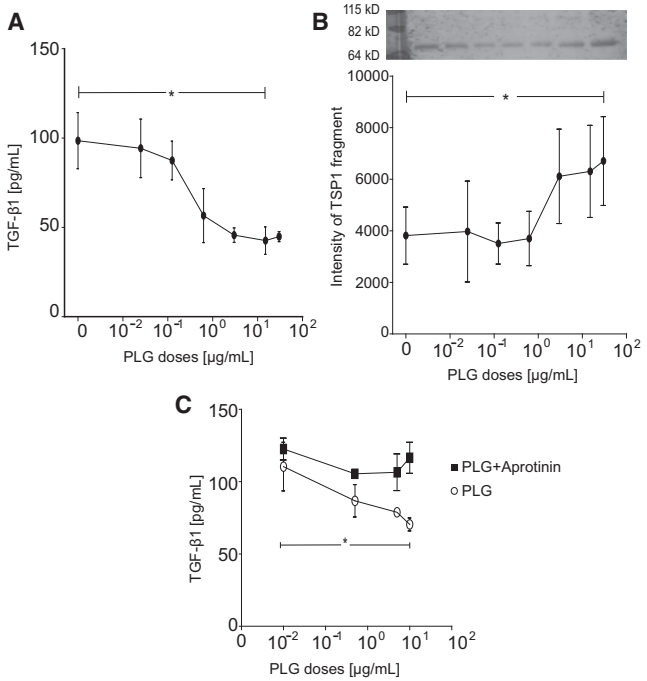

FIGURE 5 PLG addition causes a switch in TGF-β1 levels in coculture. (*A* and *B*) Different doses of PLG added to a HSC-predominant coculture of hepatocytes and T6-HSC (see Supporting Material) cause (*A*) a dose-dependent decrease in TGF-β1 protein levels and (*B*) a corresponding dose-dependent increase in TSP1 cleavage. (*C*) Addition of 1 μg/mL aprotinin together with different doses of PLG (*black squares*) does not decrease active TGF-β1 levels significantly compared with PLG alone (*open circles*; $^*p < 0.05$, $n = 3$).

PLS has a very short half-life (poor stability), and the precursor form of PLG is more stable, we administered PLG instead of PLS in the coculture. In these cocultures (which start with high levels of active TGF-β1), administering PLG caused the level of TGF-β1 to decrease (Fig. 5 *A*). Low doses of PLG (0–0.125 μg/mL) were not effective at decreasing TGF-β1, doses above the threshold of 0.125 μg/mL were capable of decreasing TGF-β1, and very high doses above 3 μg/mL caused no further decrease. Corresponding to the decrease in TGF-β1, there was also an increase in the cleavage of TSP1 (Fig. 5 *B*). The dose response of TGF-β1 to PLG was cooperative (with a Hill coefficient of 1.7), consistent with the ultrasensitivity seen in simulations. The decrease in TGF-β1 activation was due to PLS enzymatic activity, because inhibition of PLS activity using 1 μg/mL aprotinin in an HSC-predominant coculture (Fig. 5 *C*) was able to rescue the high activation state of TGF-β1.

Hysteresis in TGF-β1 activation in coculture

Given that the coculture experiments with addition of PLG showed an overall ultrasensitive decrease in TGF-β1 activation, we next sought to test the model predictions of bistability in TGF-β1. A robust indication of bistability is hysteresis, or the dependence of a system on its history (46). We tested whether the TGF-β1 levels depended on the previous system state, but instead of varying a reaction rate parameter as done in silico, we varied the PLS concentration in vitro (Supporting Material). To increase PLS, we added purified protein, and to decrease PLS, we inhibited UPA with anti-UPA mAB. Fig. S3 shows that addition of anti-UPA mAB into the HSC-predominant coculture caused PLS levels to drop to a lower steady state within 3 hr.

To test for hysteresis, we initiated the experimental model at different states by giving two treatments in an opposite order. One batch of HSC-predominant cocultures first received anti-UPA mAB to drive down PLS levels (Fig. S4 and Fig. S5), followed by addition of exogenous PLS (Fig. 6 *A*). The other batch of HSC-predominant cocultures received PLS first (Fig. S6), followed by anti-UPA treatment (Fig. 6 *B*). In both cases, we measured the final TGF-β1 levels for different doses of PLS.

If the system is monostable, then the steady-state level of TGF-β1 will depend only on the dose of PLS and not on the going-up or coming-down initialization of the system.

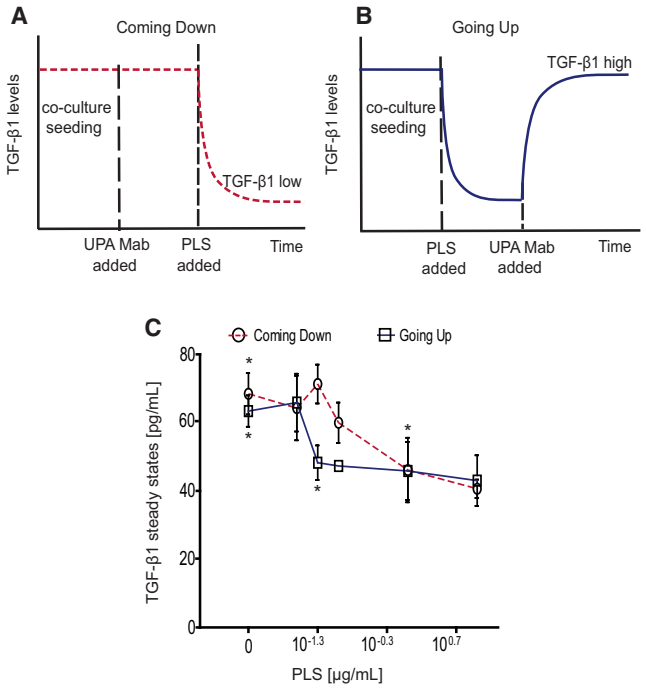

FIGURE 6 Hysteresis in TGF-β1 in coculture. (*A* and *B*) Schematic sketch of (*A*) coming-down and (*B*) going-up experimental designs (see Supporting Material). (*C*) HSC-predominant coculture was treated with anti-UPA mAB and then with different doses of PLS before TGF-β1 concentrations were measured (*dashed curve*, coming-down). HSC-predominant coculture was first treated with different doses of PLS and then treated with anti-UPA mAB before final TGF-β1 measurements were made (*solid curve*, going-up). Plotting both curves together indicates a region of TGF-β1 bistability. (Pairs of asterisks indicate significant differences with $p < 0.05$, $n = 3$.)

Coculture experiments (Fig. 6 *C*) showed that the steady-state level of TGF-β1 did not differ between the going-up and coming-down protocols for PLS doses < 50 ng/mL or > 1 μg/mL. For PLS doses between 50 ng/mL and 1 μg/mL, TGF-β1 stabilized at two different levels: a higher concentration in coming-down cocultures and a lower concentration in going-up cocultures. The experimental system exhibited two steady states of TGF-β1, with hysteresis. Both in silico modeling and coculture experiments showed a cooperative dose response for the TGF-β1 transition, and bistability for TGF-β1 activation.

DISCUSSION

To investigate the possible roles of PLS in TGF-β1 activation, we constructed a mathematical model of signaling dynamics (Fig. 1 *A*) including activation of TGF-β1 by PLS and TSP1, TGF-β1-dependent gene expression to regulate PLS and TSP1, and interplay between PLS and TSP1. When TSP1 levels are low, PLS is an activator of TGF-β1; however, adding PLS to a system with high TSP1 levels caused a decrease in TGF-β1 activation. The ability of PLS to decrease the net activation of TGF-β1 might seem to contradict the notion that PLS is an activator of TGF-β1; however, the simulated effect occurred because PLS was catalytically degrading another (stronger) activator, TSP1.

PLS and TSP1 were previously shown to antagonize each other in limited cell-free work (23,42), and our work in silico and in vitro shows the significance of this effect for TGF-β1 regulation. The simulations indicate that sufficiently high concentrations of PLS are capable of cleaving TSP1 and blunting the positive feedback loop between TSP1 and TGF-β1 (Figs. 2 and 3). When the TSP1-TGF-β1 feedback signal strength is moderate, increasing PLS will cause a decrease in TSP1 levels and a decrease in TGF-β1 (Fig. 3 *B*). However, if the positive feedback rate for TSP1 production is very high, TSP1 concentrations will become high enough that small amounts of PLS-induced cleavage will be unable to undermine the TGF-β1 high regime. Similar results were seen in vitro with an HSC predominant coculture (TGF-β1 high, PLS low), i.e., lower doses of PLS were unable to effect a switch in TGF-β1, whereas higher doses caused a significant decrease of TGF-β1 (Fig. 6). This indicates that PLS can function to antagonize TGF-β1 activation in a TSP1-rich environment.

The model-based prediction that PLG/PLS is capable of decreasing active TGF-β1 was validated in a coculture of hepatocytes and T6-HSC (Figs. 5 and 6). Single-cell approaches have been shown to be valuable for demonstrating bistability in populations of intracellular systems (47); however, our work demonstrates bistability in the extracellular environment caused by an interplay between secreted factors from multiple cell types. PLG addition caused a significant decrease in active TGF-β1 levels, accompanied by increased cleavage of TSP1, with a sigmoidal dose response. Further experiments showed that the system exhibited hysteresis, because 1), memory of the TGF-β1-low/PLS-high steady state was retained (Fig. 6 *C*, *dashed curve*) even when the endogenous PLS activation was disrupted by anti-UPA treatment (Fig. S4); and 2), memory of the TGF-β1-high/PLS-low state (Fig. 6 *C*, *solid curve*) was retained even after PLS addition. A system with mere cooperativity would have remembered only one steady state. Bistability in vitro is observed between 0.1 and 3 μg/mL of PLG, whereas PLG levels in vivo have been measured to be ~0.2 μg/mL (48). The amount of PLG needed for bistability is therefore comparable to the levels known to occur physiologically.

PLS is an activator of TGF-β1 when TSP1 levels are extremely low, as shown in Fig. 3 *B* and in previous reports in vitro (15) and in vivo (49) (Hong-Hua Mu, University of Utah School of Medicine, personal communication, 2011). In contrast to this positive correlation, previous in vivo work revealed a negative correlation between the PLS activation pathway and TGF-β1 signaling in hepatofibrotic rats (50), which have high levels of TSP1. A negative correlation between PLS and TGF-β1 has also been observed in other fibrotic diseases in vivo (20,21,51). Our preliminary data in vivo showed that a transient burst of cell-based PLS therapy was effective at causing prolonged regression of fibrotic phenomena (52), including a decrease in the concentrations of TGF-β1 and TSP1 (S.-M. Chua, L. Venkatraman, N. Tan, S. Chang, F. Y. Kuan, B. C. Narmada, J. J. Wang, C. H. Kang, S. S. Bhowmick, P. T. So, L. Tucker-Kellogg, and H. Yu unpublished results). A fibrotic disease condition could correspond to a monostable TGF-β1-high state, and an uninjured (or regressed) condition could correspond to a monostable low state. After injury, bistability could coordinate orderly transitions between the phases of wound healing, such as the start and end of a fibrogenic (matrix-regenerating, TGF-β1-high) phase of regeneration. Diseases of TGF-β1 dysregulation (52–54) could drive the system away from bistable behavior and disrupt the typical regeneration trajectory.

In this study, we used mathematical modeling to delineate specific hypotheses about the interplay between the PLS pathway and the TSP1 pathway during the activation of TGF-β1, with systems-level decisions emerging from the cross talk. A negative correlation between PLS and TGF-β1 was predicted by simulations in silico, and validated by experiments in vitro. This demonstrates that antagonism between two modes of TGF-β1 activation is capable of reversing the overall effect of an activator. The bistability of TGF-β1 activation, predicted computationally and validated experimentally, implies that both the high and low states of the system are stable and self-propagating. This understanding of the bottlenecks and sensitivities may be exploited in the future for therapeutic benefit (50). For

example, the transition in TGF-β1 activation is predicted to have regions of high sensitivity and relative insensitivity, suggesting that 1), therapies targeting TGF-β1 will be more effective if administered in contexts that are already close to the ultrasensitive transition; and 2), therapies can achieve sustained effects if a transient intervention is strong enough to activate the switch. These considerations may be useful for identifying therapeutic targets and prognostic predictors in diseases with TGF-β dysregulation.

SUPPORTING MATERIAL

Supplementary Text 1, a table, seven figures, and references (63–67) are available at http://www.biophysj.org/biophysj/supplemental/S0006-3495(12)00779-5.

We thank Siow-Thing Teo for technical support, Rashidah Sakban and Rui Rui Jia for isolation of rat hepatocytes, and Drs. Scott Friedman and Lang Zhuo for the T6-HSC cell line.

This work was supported in part by the Institute of Bioengineering and Nanotechnology, BMRC, A*STAR, ARC, NMRC, Janssen Cilag, SMA, SMART and Mechanobiology Institute of Singapore to H.Y.U.; by a Lee Kuan Yew Fellowship to L.T.K.; and by Singapore-MIT Alliance (Computational Systems Biology Programme) IUP grants to L.T.K., J.K.W., S.S.B., and C.F.D.

REFERENCES

1. Kisseleva, T., and D. A. Brenner. 2008. Mechanisms of fibrogenesis. *Exp. Biol. Med. (Maywood).* 233:109–122.
2. Reeves, W. B., and T. E. Andreoli. 2000. Transforming growth factor β contributes to progressive diabetic nephropathy. *Proc. Natl. Acad. Sci. USA.* 97:7667–7669.
3. Padua, D., and J. Massagué. 2009. Roles of TGFβ in metastasis. *Cell Res.* 19:89–102.
4. Blobe, G. C., W. P. Schiemann, and H. F. Lodish. 2000. Role of transforming growth factor β in human disease. *N. Engl. J. Med.* 342:1350–1358.
5. Shankaran, H., and H. S. Wiley. 2008. Smad signaling dynamics: insights from a parsimonious model. *Sci. Signal.* 1:pe41.
6. Schmierer, B., A. L. Tournier, …, C. S. Hill. 2008. Mathematical modeling identifies Smad nucleocytoplasmic shuttling as a dynamic signal-interpreting system. *Proc. Natl. Acad. Sci. USA.* 105:6608–6613.
7. Annes, J. P., J. S. Munger, and D. B. Rifkin. 2003. Making sense of latent TGFβ activation. *J. Cell Sci.* 116:217–224.
8. Dabovic, B., and D. B. Rifkin. 2008. TGF-β bioavailability: latency, targeting and activation. *In* The TGF-β Family. R. Derynck and K. Miyazono, editors. Cold Spring Harbor Laboratory Press, Long Island, NY. 1114.
9. Bornstein, P. 2001. Thrombospondins as matricellular modulators of cell function. *J. Clin. Invest.* 107:929–934.
10. Crawford, S. E., V. Stellmach, …, N. Bouck. 1998. Thrombospondin-1 is a major activator of TGF-β1 in vivo. *Cell.* 93:1159–1170.
11. Hugo, C. 2003. The thrombospondin 1-TGF-β axis in fibrotic renal disease. *Nephrol. Dial. Transplant.* 18:1241–1245.
12. Kondou, H., S. Mushiake, …, K. Ozono. 2003. A blocking peptide for transforming growth factor-β1 activation prevents hepatic fibrosis in vivo. *J. Hepatol.* 39:742–748.
13. Sajid, M., M. Lele, and G. A. Stouffer. 2000. Autocrine thrombospondin partially mediates TGF-β1-induced proliferation of vascular smooth muscle cells. *Am. J. Physiol. Heart Circ. Physiol.* 279: H2159–H2165.
14. Mimura, Y., H. Ihn, …, K. Tamaki. 2005. Constitutive thrombospondin-1 overexpression contributes to autocrine transforming growth factor-β signaling in cultured scleroderma fibroblasts. *Am. J. Pathol.* 166:1451–1463.
15. Lyons, R. M., L. E. Gentry, …, H. L. Moses. 1990. Mechanism of activation of latent recombinant transforming growth factor β1 by plasmin. *J. Cell Biol.* 110:1361–1367.
16. Bohmfalk, J. F., and G. M. Fuller. 1980. Plaminogen is synthesized by primary cultures of rat hepatocytes. *Science.* 209:408–410.
17. Drixler, T. A., J. M. Vogten, …, I. H. Borel Rinkes. 2003. Plasminogen mediates liver regeneration and angiogenesis after experimental partial hepatectomy. *Br. J. Surg.* 90:1384–1390.
18. Michalopoulos, G. K. 2007. Liver regeneration. *J. Cell. Physiol.* 213:286–300.
19. Lijnen, H. R. 2005. Pleiotropic functions of plasminogen activator inhibitor-1. *J. Thromb. Haemost.* 3:35–45.
20. Martínez-Rizo, A., M. Bueno-Topete, …, J. Armendáriz-Borunda. 2010. Plasmin plays a key role in the regulation of profibrogenic molecules in hepatic stellate cells. *Liver Int.* 30:298–310.
21. Huang, Y., M. Haraguchi, …, N. A. Noble. 2003. A mutant, noninhibitory plasminogen activator inhibitor type 1 decreases matrix accumulation in experimental glomerulonephritis. *J. Clin. Invest.* 112:379–388.
22. Bonnefoy, A., and C. Legrand. 2000. Proteolysis of subendothelial adhesive glycoproteins (fibronectin, thrombospondin, and von Willebrand factor) by plasmin, leukocyte cathepsin G, and elastase. *Thromb. Res.* 98:323–332.
23. Hogg, P. J., J. Stenflo, and D. F. Mosher. 1992. Thrombospondin is a slow tight-binding inhibitor of plasmin. *Biochemistry.* 31:265–269.
24. Vilar, J. M., R. Jansen, and C. Sander. 2006. Signal processing in the TGF-β superfamily ligand-receptor network. *PLOS Comput. Biol.* 2:e3.
25. Aldridge, B. B., J. M. Burke, …, P. K. Sorger. 2006. Physicochemical modelling of cell signalling pathways. *Nat. Cell Biol.* 8:1195–1203.
26. Bhalla, U. S., and R. Iyengar. 1999. Emergent properties of networks of biological signaling pathways. *Science.* 283:381–387.
27. Yao, G., T. J. Lee, …, L. You. 2008. A bistable Rb-E2F switch underlies the restriction point. *Nat. Cell Biol.* 10:476–482.
28. Novak, B., J. J. Tyson, …, A. Csikasz-Nagy. 2007. Irreversible cell-cycle transitions are due to systems-level feedback. *Nat. Cell Biol.* 9:724–728.
29. Venkatraman, L., H. Li, …, L. Tucker-Kellogg. 2011. Steady states and dynamics of urokinase-mediated plasmin activation in silico and in vitro. *Biophys. J.* 101:1825–1834.
30. Ellis, V., M. F. Scully, and V. V. Kakkar. 1987. Plasminogen activation by single-chain urokinase in functional isolation. A kinetic study. *J. Biol. Chem.* 262:14998–15003.
31. Lucas, M. A., D. L. Straight, …, P. A. McKee. 1983. The effects of fibrinogen and its cleavage products on the kinetics of plasminogen activation by urokinase and subsequent plasmin activity. *J. Biol. Chem.* 258:12171–12177.
32. Lijnen, H. R., B. Van Hoef, …, D. Collen. 1989. The mechanism of plasminogen activation and fibrin dissolution by single chain urokinase-type plasminogen activator in a plasma milieu in vitro. *Blood.* 73:1864–1872.
33. Chen, C., J. Cui, …, P. Shen. 2007. Modeling of the role of a Bax-activation switch in the mitochondrial apoptosis decision. *Biophys. J.* 92:4304–4315.
34. Cui, J., C. Chen, …, P. Shen. 2008. Two independent positive feedbacks and bistability in the Bcl-2 apoptotic switch. *PLoS ONE.* 3:e1469.
35. Reference deleted in proof.

36. Murphy-Ullrich, J. E., and M. Poczatek. 2000. Activation of latent TGF-β by thrombospondin-1: mechanisms and physiology. *Cytokine Growth Factor Rev.* 11:59–69.

37. Kutz, S. M., J. Hordines, …, P. J. Higgins. 2001. TGF-β1-induced PAI-1 gene expression requires MEK activity and cell-to-substrate adhesion. *J. Cell Sci.* 114:3905–3914.

38. Cubellis, M. V., T. C. Wun, and F. Blasi. 1990. Receptor-mediated internalization and degradation of urokinase is caused by its specific inhibitor PAI-1. *EMBO J.* 9:1079–1085.

39. Thorsen, S., M. Philips, …, B. Astedt. 1988. Kinetics of inhibition of tissue-type and urokinase-type plasminogen activator by plasminogen-activator inhibitor type 1 and type 2. *Eur. J. Biochem.* 175:33–39.

40. Ellis, V., M. F. Scully, and V. V. Kakkar. 1989. Plasminogen activation initiated by single-chain urokinase-type plasminogen activator. Potentiation by U937 monocytes. *J. Biol. Chem.* 264:2185–2188.

41. Christensen, U., and L. Sottrup-Jensen. 1984. Mechanism of α2-macroglobulin-proteinase interactions. Studies with trypsin and plasmin. *Biochemistry.* 23:6619–6626.

42. Anonick, P. K., J. K. Yoo, …, S. L. Gonias. 1993. Characterization of the antiplasmin activity of human thrombospondin-1 in solution. *Biochem. J.* 289:903–909.

43. Chen, C., J. Cui, …, P. Shen. 2007. Robustness analysis identifies the plausible model of the Bcl-2 apoptotic switch. *FEBS Lett.* 581:5143–5150.

44. Wen, F., S. Chang, …, H. Yu. 2008. Development of dual-compartment perfusion bioreactor for serial coculture of hepatocytes and stellate cells in poly(lactic-co-glycolic acid)-collagen scaffolds. *J. Biomed. Mater. Res. B Appl. Biomater.* 87:154–162.

45. Abu-Absi, S. F., L. K. Hansen, and W. S. Hu. 2004. Three-dimensional co-culture of hepatocytes and stellate cells. *Cytotechnology.* 45: 125–140.

46. Pomerening, J. R., E. D. Sontag, and J. E. Ferrell, Jr. 2003. Building a cell cycle oscillator: hysteresis and bistability in the activation of Cdc2. *Nat. Cell Biol.* 5:346–351.

47. Albeck, J. G., J. M. Burke, …, P. K. Sorger. 2008. Quantitative analysis of pathways controlling extrinsic apoptosis in single cells. *Mol. Cell.* 30:11–25.

48. Collen, D., G. Tytgat, …, P. Wallén. 1972. Metabolism of plasminogen in healthy subjects: effect of tranexamic acid. *J. Clin. Invest.* 51:1310–1318.

49. Hertig, A., J. Berrou, …, E. Rondeau. 2003. Type 1 plasminogen activator inhibitor deficiency aggravates the course of experimental glomerulonephritis through overactivation of transforming growth factor β. *FASEB J.* 17:1904–1906.

50. Zhang, W., L. Tucker-Kellogg, …, H. Yu. 2010. Cell-delivery therapeutics for liver regeneration. *Adv. Drug Deliv. Rev.* 62:814–826.

51. Nicholas, S. B., E. Aguiniga, …, W. A. Hsueh. 2005. Plasminogen activator inhibitor-1 deficiency retards diabetic nephropathy. *Kidney Int.* 67:1297–1307.

52. Bissell, D. M., D. Roulot, and J. George. 2001. Transforming growth factor β and the liver. *Hepatology.* 34:859–867.

53. Friedman, S. L., G. Yamasaki, and L. Wong. 1994. Modulation of transforming growth factor β receptors of rat lipocytes during the hepatic wound healing response. Enhanced binding and reduced gene expression accompany cellular activation in culture and in vivo. *J. Biol. Chem.* 269:10551–10558.

54. Roulot, D., A. M. Sevcsik, …, S. Marullo. 1999. Role of transforming growth factor β type II receptor in hepatic fibrosis: studies of human chronic hepatitis C and experimental fibrosis in rats. *Hepatology.* 29:1730–1738.

55. Anonick, P. K., B. Wolf, and S. L. Gonias. 1990. Regulation of plasmin, miniplasmin, and streptokinase-plasmin complex by α2-antiplasmin, α2-macroglobulin, and antithrombin III in the presence of heparin. *Thromb. Res.* 59:449–462.

56. Travis, J., and G. S. Salvesen. 1983. Human plasma proteinase inhibitors. *Annu. Rev. Biochem.* 52:655–709.

57. Eissing, T., H. Conzelmann, …, P. Scheurich. 2004. Bistability analyses of a caspase activation model for receptor-induced apoptosis. *J. Biol. Chem.* 279:36892–36897.

58. Bagci, E. Z., Y. Vodovotz, …, I. Bahar. 2006. Bistability in apoptosis: roles of bax, bcl-2, and mitochondrial permeability transition pores. *Biophys. J.* 90:1546–1559.

59. Köhler, M., S. Sen, C. Miyashita, R. Hermes, G. Pindur, M. Heiden, G. Berg, S. Mörsdorf, G. Leipnitz, M. Zeppezauer…, 1991. Half-life of single-chain urokinase-type plasminogen activator (scu-PA) and two-chain urokinase-type plasminogen activator (tcu-PA) in patients with acute myocardial infarction. *Thromb. Res.* 62:75–81.

60. Legewie, S., N. Blüthgen, and H. Herzel. 2006. Mathematical modeling identifies inhibitors of apoptosis as mediators of positive feedback and bistability. *PLOS Comput. Biol.* 2:e120.

61. Robbins, K. C., and L. Summaria. 1970. Human plasminogen and plasmin. *Methods Enzymol.* 19:184–199.

62. Saito, K., M. Nagashima, …, A. Takada. 1990. The concentration of tissue plasminogen activator and urokinase in plasma and tissues of patients with ovarian and uterine tumors. *Thromb. Res.* 58:355–366.

63. Riccalton-Banks, L., R. Bhandari, …, K. M. Shakesheff. 2003. A simple method for the simultaneous isolation of stellate cells and hepatocytes from rat liver tissue. *Mol. Cell. Biochem.* 248:97–102.

64. Vogel, S., R. Piantedosi, …, W. S. Blaner. 2000. An immortalized rat liver stellate cell line (HSC-T6): a new cell model for the study of retinoid metabolism in vitro. *J. Lipid Res.* 41:882–893.

65. Couto, L. T., J. L. Donato, and G. de Nucci. 2004. Analysis of five streptokinase formulations using the euglobulin lysis test and the plasminogen activation assay. *Braz. J. Med. Biol. Res.* 37:1889–1894.

66. Seth, D., P. J. Hogg, …, P. S. Haber. 2008. Direct effects of alcohol on hepatic fibrinolytic balance: implications for alcoholic liver disease. *J. Hepatol.* 48:614–627.

67. Stephens, R. W., J. Pöllänen, …, A. Vaheri. 1989. Activation of pro-urokinase and plasminogen on human sarcoma cells: a proteolytic system with surface-bound reactants. *J. Cell Biol.* 108:1987–1995.